Indian Journal of Chemistry
Vol. 46A, August 2007, pp. 1277-1282

Preparation, crystal structure and thermal decomposition of phenylenediammonium dichloride salts[†]

Inder Pal Singh Kapoor, Pratibha Srivastava & Gurdip Singh*

Department of Chemistry, DDU Gorakhpur University, Gorakhpur 273 009, India

Email: gsingh4us@yahoo.com

&

Roland Fröhlich

Organisch-Chemisches Institut, Universität Münster, D-48149 Münster, Germany

Received 24 November 2006; revised 6 June 2007

Phenylene-1,2-diammonium dichloride (P-1,2-DADCl), phenylene-1,3-diammonium dichloride (P-1,3-DADCl), phenylene-1,4-diammonium dichloride (P-1,4-DADCl) and 5-carboxyl-phenylene-1,3-diammonium dichloride (5-carboxyl-P-1,3-DADCl) salts have been prepared and characterized by elemental, spectral, gravimetric and X-ray crystallography. Thermal decomposition of these salts has been studied by TG and DSC and shows involvement of proton transfer as a primary step. Kinetic analysis of TG data has been evaluated by model fitting method and model free isoconversional methods.

Recently, preparation, characterization and thermal studies of a number of ring (mono- and di-) substituted arylammonium chlorides have been reported[1-5] which involves simultaneous sublimation/decomposition process. These studies are very significant since alkyl and arylammonium chlorides are generally used as phase transfer catalyst and corrosion inhibitors[6]. Studies on phenylenediammonium dichloride are not reported in the literature. Thus, in the light of these findings, we have prepared and characterized phenylenediammonium dichloride (PDADCl) salts. Thermoanalytical techniques can provide important measure of the overall kinetics of the thermally simulated reaction which permits a deeper insight into the mechanism of solid state decomposition reactions. The thermal decomposition of these chlorides has been undertaken by thermoanalytical techniques (TG and DSC) in order to understand the mechanism of decomposition. Decomposition pathway and kinetic analysis of thermal decomposition of PDADCl by the model fitting methods has also been reported. Moreover, in order to get a better understanding of the stability and decomposition process of PDADCl, we have prepared the single crystal[7-11] of phenylene-1, 2-diammonium dichloride to determine the crystal structure from X-ray diffraction data. Because of amorphous nature of the rest of the three salts phenylene-1,3-diammonium dichloride (P-1,3-DADCl), phenylene-1,4-diammonium dichloride (P-1,4-DADCl) and 5-carboxyl-phenylene-1,3-diammonium dichloride (5-carboxyl-P-1,3-DADCl), their crystallographic study could not be taken.

Experimental

Phenylene-1,2-diamine (SD Fine), phenylene-1,4-diamine (SD Fine), phenylene-1,3-diamine (Alfa aesar) and phenylene-3,5-diaminobenzoic acid (Merck) were purified by recrystallisation. HCl, $AgNO_3$ and silica gel were used as received.

All the four PDADCl salts were prepared by reacting the corresponding amines with 20% HCl in 1:2 molar ratios at room temperature as shown in Scheme 1.

The precipitated salts were dried and then washed with ethyl acetate, followed by recrystallization from distilled water. The purity of the salts was checked by TLC and their corresponding R_f values are reported in Table 1 along with physical, elemental and spectral parameters.

The salt (200 mg each) was dissolved in 150 ml of water and to this was added 0.5 ml conc. HNO_3.

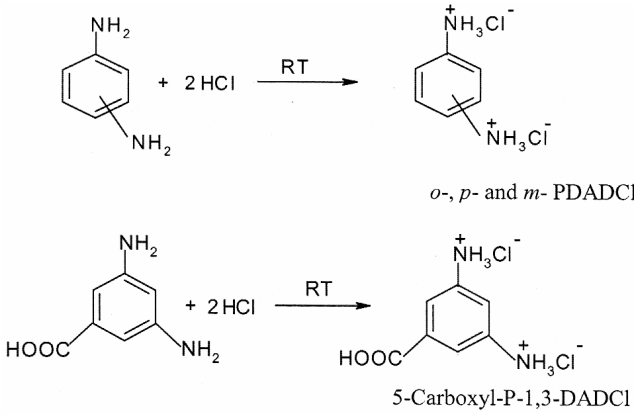

Scheme 1

[†]Part-51

Thereafter, $AgNO_3$ was added until precipitation was complete. The precipitate was filtered of in a sintered glass crucible, washed with ice cold water and dried in hot air oven. Percentage of Cl^- in each salt is given in Table 1.

The C, H, N analysis was carried out with Heraeus Carlo Erba 1108 instrument. Percentage of each element with an accuracy of ± 2%, is given in Table 1 while IR spectra were obtained on a Nicolet IR 300 spectrometer (Table 1).

Crystals of phenylene-1,2-diammonium dichloride (P-1,2-DADCl) were obtained by recrystallization from the aqueous solution. Data collection on the crystal was performed at low temperature (198 K) using a Nonius Kappa CCD diffractometer equipped with a rotatory anode generator Nonius FR 591[12]. The following programs were used: Data collection: Collect (Nonius B.V.1998), Data reduction: Denzo-SMN[13] (Otwinowski and Minor, 1997). The structure was solved by direct methods (program SHELXS-97[14]) and refined by full matrix least squares method on all F^2 data using SHELXS-97. Hydrogen atoms were placed in geometrically calculated positions (C-H= 0.93-0.97Å) and refined using a riding model. Refinement with anisotropic thermal parameters for non-hydrogen atoms led to the R-value of 0.033. The crystal structure of the P-1, 2-DADCl is shown in Fig. 1, while details of the analysis of crystal parameters, bond distances and bond angles are given in Table 2.

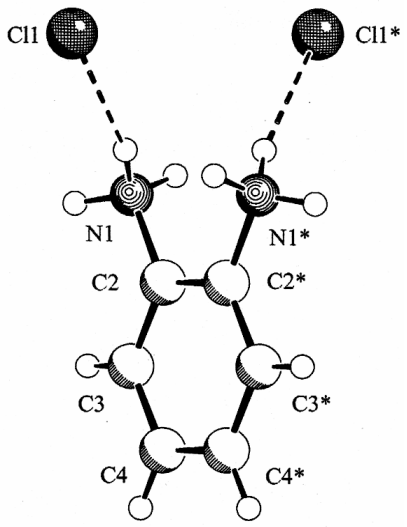

Fig. 1—Crystal structure of P-1,2-DADCl.

Table 1—Physical, elemental and spectral parameters of PDADCl salts

Comp.	Colour	Structural formula	R_f	M.pt./ decomp. (°C)	Found (Calc.) (%) C	H	N	Cl	IR data
P-1,2-DADCl	Pink crystals	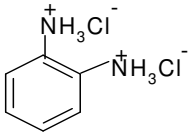	0.92	200(d)	39.12 (39.78)	4.97 (5.52)	16.03 (15.47)	39.11 (39.23)	3410(pri.aminesalt),2832; υ(C-H), 1530; υ(N-H),1503; υ(C=C), 1106; υ (C-C),870;δ(N-H)
P-1,4-DADCl	Grey amorphous	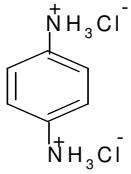	0.93	192(d)	38.73 (39.78)	5.94 (5.52)	14.53 (15.47)	38.56 (39.23)	3362(pri.aminesalt),2848; υ(C-H), 1575;υ(N-H), 1412;υ(C=C), 1112; υ (C-C) ,829;δ(N-H)
P-1,3-DADCl	Black amorphous	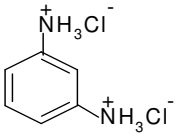	0.95	171(d)	40.32 (39.78)	4.31 (5.52)	16.23 (15.47)	38.64 (39.23)	3374(pri.aminesalt), 2836; υ(C-H), 1536; υ(N-H), 1485;υ(C=C), 1112; υ (C-C) , 771;δ(N-H)
5-carboxyl-P-1,3-DADCl	Brown amorphous	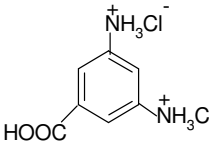	0.92	185(d)	38.35 (37.33)	5.03 (4.44)	11.34 (12.44)	30.89 (31.56)	3510(pri.aminesalt), 2889; υ(C-H), 1501; υ(N-H), 1560; υ(C=C), 1108; υ (C-C), 827; δ(N-H)

R_f= Retention factor, Eluent: a=H_2O, b =*n*-BuOH, c=gl. AcOH, d=DMSO, Locating reagent: iodine

Thermal studies

Non-isothermal TG studies on these chlorides (mass: 33 mg, 100-200 mesh) were undertaken in static air at a heating rate of 10°C min^{-1} using indigenously fabricated TG apparatus[15]. Pt crucible was used as sample holder.

TG studies on PDADCl were undertaken in nitrogen atmosphere at a heating rate using 10°C min^{-1} on thermal analyzer (TA) Q 50 and data are summarized in Table 3.

The isothermal TG studies on these chlorides (mass: 33 mg, 100-200 mesh) were carried out in static air using the above TG apparatus at appropriate temperatures (Fig. 2). Kinetic analysis from the isothermal TG data has been carried out using methods, model fitting as well as model free isoconversional. Dependencies of activation energy (E_a) on the extent of conversion (α) for the chloride salts are shown in Fig. 3.

Table 2—Crystal data, structure refinement, bond lengths and bond angles for P-1,2-DADCl

Empirical formula	$C_6H_{10}Cl_2N_2$	*Bond lengths*	
Formula weight	181.06	N(1)-C(2)	1.462(2)
Temperature	198(2) K	C(2)-C(3)	1.382(2)
Wavelength	0.71073 Å	C(2)-C(2)#1	1.393(3)
Crystal system, space group	monoclinic,	C(3)-C(4)	1.391(2)
	C2/c (No.15)	C(4)-C(4)#1	1.388(4)
Unit cell dimensions	a = 7.307(1) Å	*Bond angles*	
	b = 14.516(1) Å	C(3)-C(2)-C(2)#1	120.3(1)
	β = 94.50(1)°.	C(3)-C(2)-N(1)	118.8(1)
	c = 7.969(1) Å	C(2)#1-C(2)-N(1)	120.9(1)
Volume	842.65(17) $Å^3$	C(2)-C(3)-C(4)	119.6(2)
Z, Calculated density	4, 1.427 Mg/m^3	C(4)#1-C(4)-C(3)	120.2(1)
Absorption coefficient	0.698 mm^{-1}	Symmetry transformations used	
F(000)	376	to generate equivalent atoms:	
Crystal size	0.60 × 0.30 × 0.15 mm	#1 -x,y,-z+3/2	
θ range for data collection	2.81 to 27.86°.		
Limiting indices	-7<=h<=9, -18<=k<=16, -9<=l<=10		
Reflections collected/unique	2609/992 [R(int) = 0.0636]		
Completeness to θ = 27.86	97.7%		
Absorption correction	Multi-scan		
Max. and min. transmission	0.9025 and 0.6795		
Refinement method	Full-matrix least-squares on F^2		
Data/restraints/parameters	992/0/47		
Goodness-of-fit on F^2	1.029		
Final R indices [I>2σ(I)]	R1 = 0.0332, wR^2 = 0.0762		
R indices (all data)	R1 = 0.0435, wR^2 = 0.0789		
Largest diff. peak and hole	0.303 and -0.242 $eÅ^{-3}$		
CCDC No.	631739		

Table 3—TG and DSC data of PDADCl salts

Comp.	TG						DSC peak temp. (°C)	
	N_2 atm			Static air			Exo	Endo
	T_i (°C)	T_f (°C)	α	T_i (°C)	T_f (°C)	α		
P-1,2-DADCl	120	250	78	190	410	81	127	200
P-1,4-DADCl	140	230	82	227	450	79	119	224
P-1,3-DADCl	85	240	75	105	452	78	144	168
5-Carboxyl-P-1,3-DADCl	85	260	65	208	550	65	122	226

T_i = Initial temp. , T_f = Final temp., α = Percent decomposition

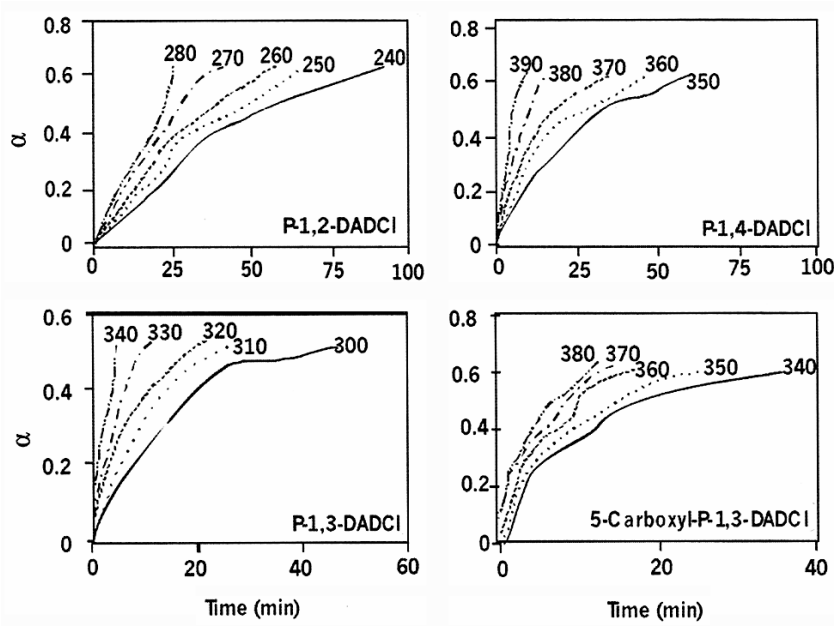

Fig. 2—Isothermal TG curves of PDADCl salts (Temp. in °C).

DSC studies on PDADCl were undertaken in inert atmosphere (nitrogen flow at a rate of 50 ml min^{-1}) on a 2010 TA instrument (sample mass: 20 mg, heating rate 10°C min^{-1}) and data are summarized in Table 3.

Kinetic analysis of isothermal TG data

Kinetic analysis of solid state decomposition is usually based on a single step kinetic equation,

$$d\alpha/dt = k\,(T)\,f\,(\alpha) \quad \ldots\ (1)$$

where t is the time, T is the temperature, α is the extent of conversion ($0 < \alpha < 1$), $k\,(T)$ is the rate constant and f (α) is the reaction model which describes the dependence of the reaction rate on the extent of reactions. The value of α is experimentally derived from the global mass loss in TG experiments. The reaction model may take various forms, some of which are shown in Table 4. The temperature dependence of rate constant $k\,(T)$ can be satisfactorily described by the Arrhenius Eq., whose substitution into Eq. (1) yields:

$$d\alpha/dt = A \exp(-E_a/RT).f\,(\alpha) \quad \ldots\ (2)$$

where A is pre-exponential factor, E_a is activation energy and R is the gas constant.

Model fitting method

Rearrangement and integration of Eq. (1) for isothermal conditions gives

$$g_j\,(\alpha) = k_j\,(T)\,t \quad \ldots\ (3)$$

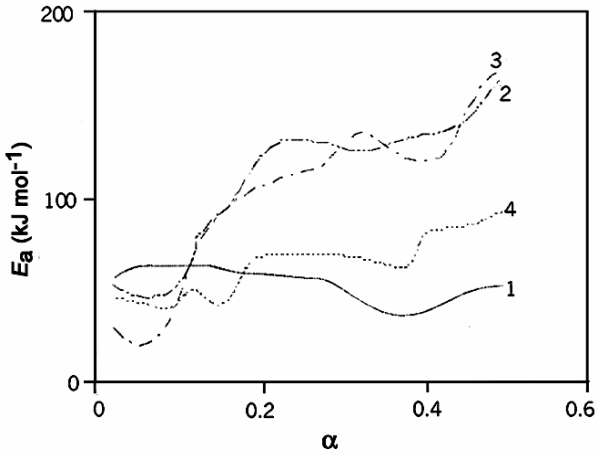

Fig. 3—Dependencies of activation energy (E_a) on the extent of conversion (α) for 1. P-1,2-DADCl, 2. P-1,4-DADCl, 3. P-1,3-DADCl, 4. 5-Carboxyl-P-1,3-DADCl.

where $g\,(\alpha) = {}_0\int^{\alpha} [f\,(\alpha)]^{-1}\,d\alpha$ is the integrated form of the reaction model (Table 4). The subscript j has been introduced to emphasize that substituting a particular reaction model in Eq. (3) results in evaluating the corresponding rate constant, which is determined from the slope of plot of $g_j\,(\alpha)$ versus t. For each reaction model selected, the rate constants are evaluated at several temperatures T_i and Arrhenius parameters are determined using the Arrhenius equation, Eq. (4), in its logarithmic form:

$$\ln k_j\,(T_i) = \ln A_j - E_j/RT_i \quad \ldots\ (4)$$

Table 4—Reaction models applied to describe thermal decomposition of solids

Model no.	Reaction model	f(α)	g(α)
1	Power law	$4\,\alpha^{3/4}$	$\alpha^{1/4}$
2	Power law	$3\,\alpha^{2/3}$	$\alpha^{1/3}$
3	Power law	$2\,\alpha^{1/2}$	$\alpha^{1/2}$
4	Power law	$2/3\,\alpha^{-1/2}$	$\alpha^{3/2}$
5	One-dimensional diffusion	$1/2\,\alpha^{-1}$	α^{2}
6	Mampel (first order)	$1-\alpha$	$-\ln(1-\alpha)$
7	Avrami-Erofeev	$4(1-\alpha)[-\ln(1-\alpha)]^{3/4}$	$[-\ln(1-\alpha)]^{1/4}$
8	Avrami-Erofeev	$3(1-\alpha)[-\ln(1-\alpha)]^{2/3}$	$[-\ln(1-\alpha)]^{1/3}$
9	Avrami-Erofeev	$2(1-\alpha)[-\ln(1-\alpha)]^{1/2}$	$[-\ln(1-\alpha)]^{1/2}$
10	Contracting sphere	$3(1-\alpha)^{2/3}$	$1-(1-\alpha)^{1/3}$
11	Three-dimensional diffusion	$2(1-\alpha)^{2/3}[1-(1-\alpha)^{1/3}]^{-1}$	$[1-(1-\alpha)^{1/3}]^{2}$
12	Contracting cylinder	$2(1-\alpha)^{1/2}$	$1-(1-\alpha)^{1/2}$
13	Prout-Tomkins	$\alpha\,(1-\alpha)$	$\ln(\alpha / 1-\alpha)$
14	Ginstling-Brounshtein	$3/2[(1-\alpha)^{-1/3}-1]^{-1}$	$[1-(2\,\alpha / 3)]-(1-\alpha)^{2/3}$

Table 5—Arrhenius parameters for isothermal decomposition of PDADCl salts

Model*	P-1,2-DADCl			P-1,4-DADCl			P-1,3-DADCl			5-carboxyl-P-1,3-DADCl		
	E_a (kJ/mol)	-ln A	r	E_a (kJ/mol)	-ln A	r	E_a (kJ/mol)	-ln A	r	E_a (kJ/mol)	-ln A	r
1	70.4	11.0	0.9892	178.3	28.6	0.9122	172.0	31.1	0.9836	97.2	14.6	0.9696
2	70.1	11.1	0.9894	178.0	28.7	0.9130	171.6	31.2	0.9838	97.1	14.7	0.9699
3	69.4	11.2	0.9897	177.4	28.8	0.9147	171.0	31.2	0.9842	96.8	14.8	0.9705
4	65.3	10.1	0.9917	174.8	28.4	0.9234	167.2	30.2	0.9861	95.4	14.5	0.9739
5	63.4	9.5	0.9926	174.0	28.2	0.9269	165.5	29.5	0.9867	94.7	14.2	0.9754
6	65.1	10.7	0.9918	174.8	29.1	0.9254	167.4	30.8	0.9858	95.2	15.1	0.9742
7	69.2	11.0	0.9898	177.3	28.7	0.9160	171.1	31.1	0.9840	96.7	14.7	0.9708
8	68.7	11.1	0.9900	177.0	28.9	0.9171	170.7	31.2	0.9842	96.5	14.9	0.9712
9	67.8	11.1	0.9905	176.3	29.0	0.9193	169.8	31.2	0.9847	96.2	15.1	0.9720
10	65.9	9.6	0.9915	175.1	27.9	0.9233	168.0	29.7	0.9856	95.5	13.9	0.9736
11	61.5	7.4	0.9934	173.5	26.5	0.9322	163.9	27.4	0.9869	93.9	12.4	0.9771
12	66.2	10.0	0.9913	175.3	28.2	0.9223	168.2	30.1	0.9856	95.8	14.3	0.9318
13	69.6	12.9	0.9896	177.8	30.7	0.9153	171.7	33.1	0.9835	96.9	16.6	0.9704
14	62.1	7.3	0.9932	173.6	26.3	0.9303	164.4	27.4	0.9869	94.2	12.3	0.9765

* Enumeration of the model is as given in Table 4.

Arrhenius parameters evaluated for isothermal experimental data by the model fitting method[16] are presented in Table 5.

Model free isoconversional method

The model free isoconversional method[17,18] allows the activation energy to be evaluated without making any assumptions about the reaction model. Additionally, the method evaluates the effective activation energy as a function of the extent of conversion, which allows one to explore multistep kinetics.

The basic assumption of the isoconversional method is that the reaction model as defined in Eq. (1) is not dependent on temperature or heating rate. Under isothermal conditions, on combining Eqs (3) and (4) we get Eq. (5).

$$-\ln t_{\alpha,i} = \ln [\, A_\alpha / g\,(\alpha)] - E_\alpha / RT_i \quad \ldots\ (5)$$

where E_α is evaluated from the slope of the plot of $-\ln t_{\alpha,i}$ against T_i^{-1}. Thus, E_α at various α_i for PDADCl have been evaluated and the E_α dependencies on are shown in Fig. 3.

Results and discussion

Elemental, gravimetric, spectral and X-ray crystallographic data reported in Tables 1 and 2, indicate the formation of PDADCl. DSC data show that all salts have both endotherms and exotherms. Most of the endothermic peaks correspond to melting point/sublimation of these salts. In order to confirm sublimation, each salt was separately submitted to sublimation. The salts sublime at ~120°C and each

sublime was proved as parent salt by co-TLC. It is inferred that sublimation dominates at lower temperatures and at higher temperatures, combination of significant sublimation and endothermic degradation results in the formation of gaseous products[3-5].

TG on the salts in static air and in nitrogen atmosphere show that all salts undergo about 70-80% mass loss, leaving a small amount of black residue. 5-Carboxyl-P-1,3-DADCl show two step decomposition reaction. The weight loss (20%) corresponds to the evolution of one carbon dioxide molecule and 32% weight loss shows evolution of two additional molecules.

The thermal stability of PDADCl may depend upon the tendency of arylammonium ion to release a proton to chloride ion[3-5]. Moreover, the tendency of chloride to accept proton depends on its basicity at higher temperatures. Thus, the overall decomposition process seems to commence by two routes. In the first route, the transfer of proton[2-5] through an activated complex, from arylammonium ion to chloride ion, form amine and HCl molecule in the condensed phase[2-5]. At higher temperatures, interaction between HCl and amine cause ring rupture which forms gaseous products. The reaction pathways are summarized in Scheme 2. In the second route, PDADCl may sublime to form aerosol[3-5,19] prior to decomposition (deamination, decarboxylation and ring rupture) which leads to formation of gaseous products (Scheme 2). Similar type of behaviour has also been reported for arylamine bromide salts[2-5].

Amongst various values of correlation coefficient '*r*' obtained from different models (Table 4), *r* value is highest for model 11 (Table 5), i.e., the reaction mechanism involves three-dimensional diffusion. The corresponding values of E_a are reported in Table 5 for *o*-, *p*- and *m*- isomer (61.5, 173.5 and 163.9 $kJmol^{-1}$ respectively) and for carboxylic derivative (93.9 $kJmol^{-1}$). The least value for *o*- isomer is due to steric hindrance between *o*-substituents. This also supports the contention[20] that *o*-substituted groups generally exert N-H bond weakening effect of same kind whether they are electron demanding (-I) or donating (+I). The low value of activation energy for $–CO_2H$ derivative (compared to *m*-isomer) is due to the –I effect of $–CO_2H$ group which may cause weakening of N-H bonds. The weakening of N-H bonds facilitates proton transfer reaction. This reaction occurring in the solid state is three-dimensional diffusion, as is clear from their *r* values.

Model free isoconversional method shows that the thermolysis of these salts is not as simple as indicated by model fitting methods. As can be seen from Fig. 3, the value of E_a changes with α. The variation of E_a clearly shows that there are more than one competing reaction channels during decomposition steps. The contribution of different paths to the value of E_a changes with the value of α.

The above kinetic studies of the thermal decomposition of the PDADCl salts give the order of activation energy for decomposition as follows: P-1,4-DADCl>P-1,3-DADCl>5-carboxyl-P-1,3-DADCl >P-1,2-DADCl. The thermal decomposition of PDADCl occurs principally by dissociation into HCl and corresponding amines. The results show that proton transfer reaction plays an important role in the thermal decomposition of these salts.

References

1 Singh G, Kapoor I P S & Kaur J, *Indian J Eng Mat Sci*, 7 (2000) 229.

2 Singh G, Kapoor I P S & Kaur J, *Thermochim Acta,* 351 (2000) 139.

3 Singh G, Kapoor I P S & Kaur J, *Thermochim Acta*, 338 (1999) 45.

4 Singh G, Kapoor I P S & Kaur J, *Indian J Chem*, 38B (1999) 56.

5 Singh G, Kapoor I P S & Kaur J, *J Therm Anal Cal*, 62 (2000) 305.

6 Bhalerao U T, Mathur S N & Rao S N, *Synthetic Comm*, 22 (1992) 1645.

7 Kapoor I P S, Srivastava P, Singh G & Frolich R, *Indian J Chem*, 45A (2006) 1820.

8 Singh G, Prajapati R & Fröhlich R*, J Haz Mat*, A118 (2005) 75.

9 Singh G, Singh C P & Fröhlich R, *J Therm Anal Calor,* 85 (2006) 2, 425.

10 Zhang Shusheng, Le Xuemei, Wang Jinli & Wen Yonghong, *Indian J Chem,* 43A (2004) 1444.

11 Begum N, Uttam Das K, Hossain GMG, Hyder I & Kabir SE, *Indian J Chem,* 44A (2005) 1988.

12 Hooft R, *COLLECT Data Collection Software*, (Nonius B V, Delft: The Netherlands) 1998.

13 Otwinowski Z & Minor W, *Meth Enzymol*, 276 (1997) 307.

14 Sheldrick G M, *Acta Cryst,* A46 (1990) 467.

15 Singh G & Singh R R, *Res Ind*, 23 (1978) 92.

16 Singh G, Felix S P & Pandey D K, *Thermochim Acta*, 411 (2004) 61.

17 Vyazovkin S, *Int J Chem Kinet*, 28 (1996) 95.

18 Vyazovkin S & Wight C A*, J Phys Chem A* 101(1997) 8279.

19 Patil D G, Jain S R & Brill T B, *Propellants Explosive Pyrotechnics*, 17 (1992) 99.

20 Morrison R T & Boyd R N, *Organic Chemistry*, (Prentice-Hall of India, New Delhi) 1989, p. 959.